Biochemical and Biophysical Research Communications 454 (2014) 289–294

Contents lists available at ScienceDirect

Biochemical and Biophysical Research Communications

journal homepage: www.elsevier.com/locate/ybbrc

Mutant PrP^{CJD} prevails over wild-type PrP^{CJD} in the brain of V210I and R208H genetic Creutzfeldt–Jakob disease patients

Franco Cardone [a,1,*], Serena Principe [a,1], Maria Eugenia Schininà [b,1], Bruno Maras [b], Sabina Capellari [c,d], Piero Parchi [c,d], Silvio Notari [c], Laura Di Francesco [b], Anna Poleggi [a], Roberta Galeno [a], Ramona Vinci [a], Vittorio Mellina [a], Susanna Almonti [a], Anna Ladogana [a], Maurizio Pocchiari [a]

[a] Dipartimento di Biologia Cellulare e Neuroscienze, Istituto Superiore di Sanità, Viale Regina Elena 299, 00161 Rome, Italy
[b] Dipartimento di Scienze Biochimiche, "Sapienza" University of Rome, Piazzale Aldo Moro 5, 00185 Rome, Italy
[c] Dipartimento di Scienze Biomediche e Neuromotorie, University of Bologna, Via Ugo Foscolo 7, 40123 Bologna, Italy
[d] IRCCS, Istituto delle Scienze Neurologiche, Via Altura 3, 40139 Bologna, Italy

ARTICLE INFO

Article history:
Received 2 October 2014
Available online 19 October 2014

Keywords:
gCJD
Quantitative MS
PrP^{27-30}
TSE
Amyloidogenesis
PrP allotypes

ABSTRACT

Creutzfeldt–Jakob disease (CJD) is a neurodegenerative disorder characterized by the deposition of the pathological conformer (PrP^{CJD}) of the host encoded cellular prion protein (PrP^{C}). In genetic CJD associated with V210I or R208H PrP substitutions, the pathogenic role of mutant residues is still poorly understood. To understand how V210I or R208H PrP mutations facilitate the development of the disease, we determined by mass spectrometry the quantitative ratio of mutant/wild-type PrP^{CJD} allotypes in brains from affected subjects. We found that the mutant PrP^{CJD} allotypes moderately exceeds of 2- or 3-fold the amount of the wild-type counterpart suggesting that these mutations mainly exert their pathogenic effect on the onset of the pathogenic cascade.

Different mechanisms can be hypothesized to explain the pathogenic role of mutant residues: V210I and R208H substitutions can increase the concentration of PrP^{C} and the probability to form insoluble aggregates, or they may facilitate the formation of pathological intermediates, or, alternatively, they may increase the affinity for ligands that are involved in the initial phases of PrP^{CJD} formation and aggregation.

Whatever the mechanism, the enrichment found for the mutated PrP^{CJD} species indicates that these altered structures are more prone, with respect to the non-mutated ones, to be captured in the polymerization process either at the onset or during the development of the disease.

1. Introduction

Genetic Creutzfeldt–Jakob disease (gCJD) is a mendelian-inherited neurodegenerative disorder affecting humans that belongs to the group of transmissible spongiform encephalopathies (TSEs), or prion diseases. Besides genetically transmitted syndromes (also including Gerstmann–Sträussler–Scheinker disease, GSS, and fatal familial insomnia), human TSEs comprise idiopathic (sporadic CJD and sporadic fatal insomnia) and acquired (iatrogenic and variant CJD) disorders, all of which are characterized by the formation and often deposition in the central nervous system (CNS) of the disease-specific conformer (PrP^{CJD}) of the cellular prion protein (PrP^{C}) [1].

Point or insert PrP^{C} mutations associate with genetic forms of prion diseases and, together with the polymorphic site at position 129 (encoding for either methionine or valine), influence the clinical, pathological, and biochemical phenotypes of the disease suggesting that the primary structure of PrP^{C} is important for disease development [2–6]. In silico and in vitro studies [7] suggest that some mutations (e.g. D178N, F198S) destabilise PrP^{C} increasing the probability to misfold and aggregate into nuclei of fibrillization while others, such as V210I and R208H, would have only limited effects on the stability of the protein. V210I is the second most

Abbreviations: CJD, Creutzfeldt–Jakob disease; PrP, prion protein; TSEs, transmissible spongiform encephalopathies; GSS, Gerstmann–Sträussler–Scheinker disease; *PRNP*, PrP gene; SDS–PAGE, sodium dodecyl sulphate polyacrylamide gel electrophoresis; DTT, dithiothreitol; CNBr, cyanogen bromide; TFA, trifluoroacetic acid; SIM, selected ion monitoring; LC–MS, liquid chromatography mass spectrometry.

* Corresponding author. Fax: +39 0649903012.
E-mail address: franco.cardone@iss.it (F. Cardone).
[1] Authors equally contributing to this work.

http://dx.doi.org/10.1016/j.bbrc.2014.10.051
0006-291X/

frequent mutation associated with genetic CJD [3–8] with a cumulative penetrance of about 80% (personal data), while R208H is extremely rare [2,9–11]. Despite this remarkable difference in incidence, both mutations associate with clinical, neuropathological, and biochemical features, which are virtually indistinguishable from sporadic CJD (sCJD). These findings make it difficult to determine the influence exerted by the isoleucine 210 and histidine 208 substitutions on the occurrence and the clinico-pathological phenotype of the disease.

In V210I gCJD brains, Silvestrini and colleagues [12] showed by HPLC, Edman sequencing and mass spectrometry, that both the mutant and the wild-type allotypes of PrP^{C} are converted and accumulated as insoluble and protease resistant PrP^{CJD} aggregates. In that work [12] it was hypothesized that V210I PrP^{C}, more prone to spontaneously convert into pathological aggregates, can act as the initial seed that catalyses conversion and further addition of mutant and wild-type PrP^{CJD}. Subsequent studies on cell culture models showed that mutant, aggregation prone, isoforms of PrP^{C} may effectively act as seed that recruit wild-type, soluble PrP^{C} molecules to form larger aggregates that precipitate in the cell [13], surprisingly, in V210I patients, the hypothesized preferential conversion of the mutant protein into PrP^{CJD} has never been supported by evidences obtained by direct studies of affected brains.

The aim of this work is to provide novel information useful to elucidate the role of V210I and R208H mutations in the formation of PrP^{CJD} by determining the ratio of mutated versus non-mutated allotype in PrP^{CJD} aggregates in brain tissues taken from patients carrying the corresponding mutation.

To do this we developed an improved version of our previous mass spectrometry quantitative method [14] that is now based on the use of internal controls (deuterated version of relevant peptides) and a reference calibration curve, which allowed us to accomplish the relative quantification of PrP^{CJD} allotypes accumulating in the brain of heterozygous patients with gCJD with unprecedented reliability. A clear prevalence of the mutant allotype was demonstrated in all the samples analysed, suggesting the primacy of the mutant PrP in the development of the disease.

2. Materials and methods

2.1. Patients and tissues

Brain samples from one R208H and four V210I gCJD patients were from the frozen tissue collections of the Italian National Registry of CJD at the Istituto Superiore di Sanità and the Laboratory of Neuropathology of the University of Bologna.

Data collection on CJD suspected cases is an integral part of the CJD surveillance study which was approved by the Ethical Committee of the Istituto Superiore di Sanità (prot. CE-ISS 09/266).

PRNP mutations and the polymorphism at position 129 were identified by direct sequencing of genomic DNA [8]. Details on *PRNP* genotypes and brain areas used for performing this study are reported in Table 1.

Table 1
Genetic data on gCJD patients and brain tissue used for the study.

Patient	Mutation	Residue 129	Brain region
A	R208H	M/M	Cerebral cortex
B	V210I	M/M	Cerebral cortex
B	V210I	M/M	Cerebellum
C	V210I	M/V	Cerebral cortex
D	V210I	M/M	Cerebral cortex
E	V210I	M/V	Cerebral cortex
E	V210I	M/V	Cerebellum

2.2. Purification of the protease-resistant core fragment of PrP^{CJD} ($PrP^{27–30}$) from human brain

$PrP^{27–30}$, the protease-resistant core fragment of PrP^{CJD}, was extracted from brain samples and inactivated according to published protocols [12,14,15].

Western Blotting and SDS–PAGE followed by silver staining assessed the presence and purity of $PrP^{27–30}$ in brain samples [16].

2.3. CNBr cleavage of $PrP^{27–30}$ samples and synthetic peptides

$PrP^{27–30}$ pellets were dissolved in 70% formic acid, reduced with 50 mM DTT (Sigma Aldrich) and treated with CNBr (Sigma–Aldrich). The resulting peptide mixtures include peptides 207–213, referred to as "reporter peptides", which contain residues 208 and 210 and are representative of the corresponding full-length PrP allotype.

Synthetic, non-deuterated (ERVVEQMA, E**H**VVEQMA, and ERV**I**EQMA, used as calibrants) and deuterated peptides (ERV_{d8}-VEQMA, E**H**V_{d8}VEQMA, and ERV_{d8}**I**EQMA, used as internal standards) (Inbios, Naples, Italy) were treated with CNBr to obtain 207–213 peptides with C-terminus identical to CNBr-treated $PrP^{27–30}$. Hereby, the C-ter homoserine lactone of these peptides is indicated with a methionine residue (abbreviated with a M).

2.4. LC–MS profiling of $PrP^{27–30}$allotypes

Each mixture of $PrP^{27–30}$ peptides was dissolved in 100 μl of 10% trifluoroacetic acid (TFA). Equal amounts of CNBr-treated wild-type and 210I or 208H mutant deuterated peptides were dissolved in 50 μl of 0.056% TFA and added to the corresponding $PrP^{27–30}$ sample as internal standards to determine the retention times of the corresponding $PrP^{27–30}$-derived peptides.

Each mixture was loaded onto a reversed-phase C_8 column (250 × 2.1 ID, 5 μm particle size, 300 Å pore size, Vydac, Hesperia, CA, USA) and fractionated by an HPLC apparatus (model LabFlow 4000, Bologna, Italy) on-line connected to an ion trap mass spectrometer equipped with an electrospray ion source (ES-IT, mod. LCQ, ThermoElectron, San Jose, CA, USA). The column was equilibrated with 99% solvent A (0.056% TFA) and 1% solvent B (0.05% TFA acid in 70% acetonitrile). Elution was performed at a flow rate of 150 μl/min with a linear gradient from 1% to 60% of solvent B in 60 min.

Internal standard peptides were detected by on-line monitoring of the ion currents at the m/z ranges of 829.9–832.9 (E**H**V_{d8}VEQM), 863.0–866.0 (ERV_{d8}**I**EQM) and m/z 848.9–851.9 (ERV_{d8}VEQM), whereas $PrP^{27–30}$ reporter peptides were revealed at m/z ranges 821.9–824.9 (E**H**VVEQM), 854.9–857.9 (ERV**I**EQM), and 840.9–843.9 (ERVVEQM). The elution of these peptides took place at 28% of the imposed gradient. Electrospray voltage was 4.5 kV and capillary temperature was 240 °C.

Selected ion monitoring (SIM) traces building, peak detection and peak integration were produced by the Excalibur software.

2.5. Quantification procedure

Stock solutions of synthetic peptides at increasing concentrations were made in 0.056% TFA by mixing increasing amounts of the relevant couple of reporter peptides (ERVVEQM and ERV**I**EQM for V210I mutation, or ERVVEQM and E**H**VVEQM for R208H mutation) to fixed amounts of the corresponding deuterated peptides (ERV_{D8}VEQM and ERV_{D8}**I**EQM, or ERV_{D8}VEQM and E**H**V_{D8}VEQM).

These solutions were used to build linearity curves following three different modalities of analyses. Firstly, mass spectra were acquired after loop injection of 5 μl of each solution in 150 μl/min flow rate of 28% solvent B. Secondly, human samples were

loaded in the LC–MS system and when the endogenous reporter 207–213 peptides (revealed by monitoring the parent ion current) were eluted from the column, the gradient was stopped (28% of solvent B) and 50 μl of each stock solution injected in the LC–MS apparatus at approximately 8 min intervals. Calibration curves were built from the area ratio of LC–MS peaks of calibrant and deuterated peptides (internal standards). Finally, linearity curves were built by submitting the synthetic peptide solutions to the LC–MS system soon after the analyses of purified and digested $PrP^{27–30}$ from diseased human brains. In each experiment, ions were selectively monitored at the pertinent *m/z* value using a window ±3 amu width (see above) and peak area values obtained for each measurement were normalised on the fixed amounts of the relevant internal standards and then plotted versus the corresponding peptide amounts.

3. Results

The results of Western blotting and silver staining of SDS–polyacrylamide gels showed that the procedure adopted to process brain samples removes the vast majority of cellular proteins yielding a fraction highly enriched in $PrP^{27–30}$. However, residual traces of non-PrP factors detected in these samples [17] could influence the chromatographic behaviour, the ionization efficiency of PrP peptides or both [18], causing any quantitative measurements of relevant PrP peptides poorly reliable. To overcome this difficulty, we prepared dose–response calibration curves of synthetic peptides mixed into the $PrP^{27–30}$ matrix resident in the chromatographic column [19].

The dose–response curve for PrP V210I allotypes (Fig. 1) and the *R*-coefficient values relative to the dose–response curves obtained from synthetic peptides mixed with the CNBr-cleaved $PrP^{27–30}$ from brain samples (Table 2) revealed an accurate linearity of the LC–MS setting. The accuracy of these measurements was further controlled by spiking CNBr digested $PrP^{27–30}$ extracted from gCJD brain samples with fixed amounts of deuterated peptides, which served as internal reference standards.

Mass spectrometry (SIM) traces of the reporter peptides showed that the quantity of the mutant proteins exceeds that of the wild-type counterpart with ratio of about 3–1 for the R208H samples (Fig. 2 and Table 3) and about 2–1 for the V210I samples (Fig. 3 and Table 3). For V210I samples, the observed ratios were not affected by the presence of methionine (M) or valine (V) at position 129 of the wild-type allotype, nor by the area of brain where the samples were taken.

4. Discussion

By using a specially developed quantitative analytical method, we showed here for the first time that, in the brain of V210I and R208H gCJD patients, the insoluble and PK resistant core of PrP^{CJD} contains a moderate excess of the mutant PrP allotype. We also found that the ratio between mutant and wild-type protein is comparable among the four V210I gCJD patients examined regardless of their composition at the polymorphic position 129 (129 M/M or 129 M/V), suggesting that the nature of this amino acidic residue has a negligible effect on the process of PrP^{CJD} conversion and deposition.

There are several possible mechanisms that would explain the 2 (V210I) to 3 (R208H) folds increase of mutant with respect to wild-type allotype in $PrP^{27–30}$ formation.

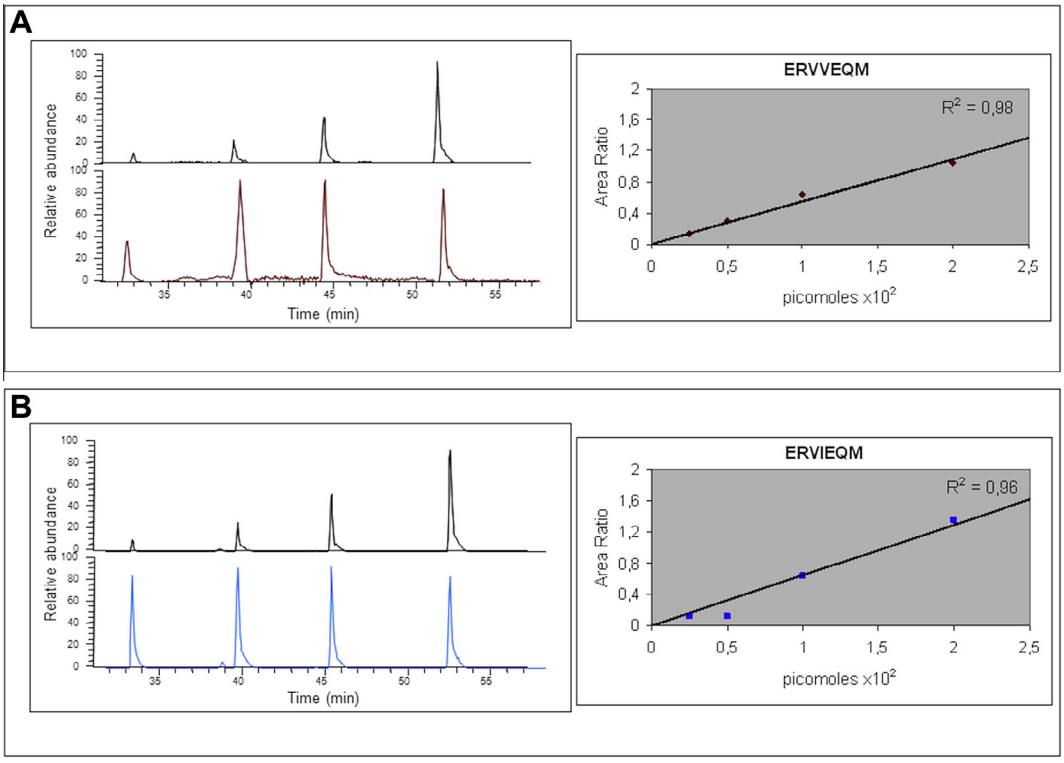

Fig. 1. Calibration curves of PrP 207–213 peptides. Linearity curves of peptides ERVVEQM and ERVIEQM. Quantitative mass spectrometric data were achieved from 50 μl of serial dilution samples (0.25–4 μM) in 0.05% TFA. Increasing amounts of each calibrating peptides, spiked with 100 pmol of the corresponding deuterated peptide as internal standard, were injected soon after the elution of the endogenous peptides proteolytically released from $PrP^{27–30}$ isolated from diseased human brain. The calibration curves were built from the ratio between the peak areas of each serial samples. Panel A: Total ion currents for all four injected calibration samples are reported, collected in a selective ion monitoring (SIM) mode at *m/z* 840.9–843.9 for the ERVVEQM peptide (upper left panel), and 848.9–851.9 for the deuterated form (lower left panel). In the right panel, the calibration curve is shown. Panel B: Total ion currents for all four injected calibration samples are reported, collected in SIM mode at *m/z* 854.9–857.9 for the ERVIEQM peptide (upper left panel), and 863.0–866.0 for the deuterated form (lower left panel). In the right panel, the calibration curve is shown.

Table 2
R^2 values of linearity curves.

PrP^{27-30} sample[a]	R^2 of mutant peptide linearity curves (H or I)[b]	R^2 of wild-type peptide linearity curves
PrP^{27-30} patient A (cereb. cortex)	0.9897 (H)	0.9913
PrP^{27-30} patient B (cereb. cortex)	0.9962 (I)	0.8334
PrP^{27-30} patient B (cerebellum)	0.8969 (I)	0.9653
PrP^{27-30} patient C (cereb. cortex)	0.9885 (I)	0.9830
PrP^{27-30} patient D (cereb. cortex)	0.9820 (I)	0.9068
PrP^{27-30} patient E (cereb. cortex)	0.9618 (I)	0.9902
PrP^{27-30} patient E (cerebellum)	0.9897 (I)	0.9887

[a] This column refers to samples whose HPLC run was stopped soon after the elution of endogenous reporter peptides and before loading stock solutions of calibrant peptides and internal standards.
[b] (H) refers to synthetic peptide EHVVEQM carrying the Arg to His mutation on the residue 208, (I) refers to synthetic peptide ERVIEQM carrying the Val to Ile mutation on the residue 210.

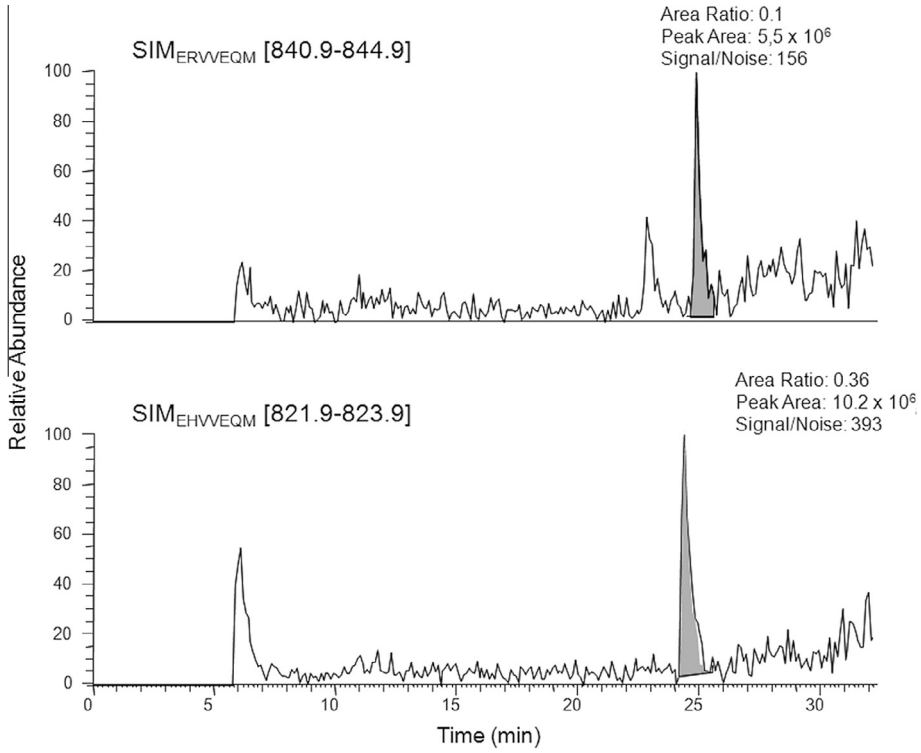

Fig. 2. Mass spectrometric detection of the human PrP^{27-30} allotypes isolated from the cerebral cortex of patient A. Detection of peptide ERVVEQM (upper panel) and EHVVEQM (lower panel) was simultaneously achieved by selectively monitoring parent ion currents (SIM mode) at m/z 840.9–844.9 and 821.9–823.9, respectively. Quantitative data are reported above SIM peak, as: (a) area ratio between the area of the endogenous PrP peptide and the spiked internal standard deuterated peptide; (b) peak area automatically achieved with same integration parameter; (c) signal to noise ratio.

Table 3
Stoichiometric ratios between mutant and wild-type PrP allotypes in PrP^{27-30} preparations.

Patient	Mutation	Residue 129	Brain region	Mutant/wild type allotype
A	R208H	M/M	Cerebral cortex	3.4/1
B	V210I	M/M	Cerebral cortex	1.6/1
B	V210I	M/M	Cerebellum	1.8/1
C	V210I	M/V	Cerebral cortex	1.9/1
D	V210I	M/M	Cerebral cortex	1.6/1
E	V210I	M/V	Cerebral cortex	1.6/1
E	V210I	M/V	Cerebellum	1.5/1

Firstly, mutant PrP^{C} allotype may have a higher local concentration in the cell than the wild-type counterpart and this could facilitate the process of protein misfolding and aggregation.

An increased cellular level can derive from a more efficient production, from a slower cellular clearance (possibly caused by a different conformation of mutant PrP^{C}), or both. To verify whether PrP^{C} allotype levels are influenced by the levels of the corresponding mRNA, we investigated the amounts of mutant and wild-type mRNA in V210I brain samples and found that they are produced within the same order of magnitude, suggesting that the mutant/wild-type PrP^{CJD} allotype ratio does not derive from unbalanced mRNAs amounts. The other hypotheses remain matter for investigation.

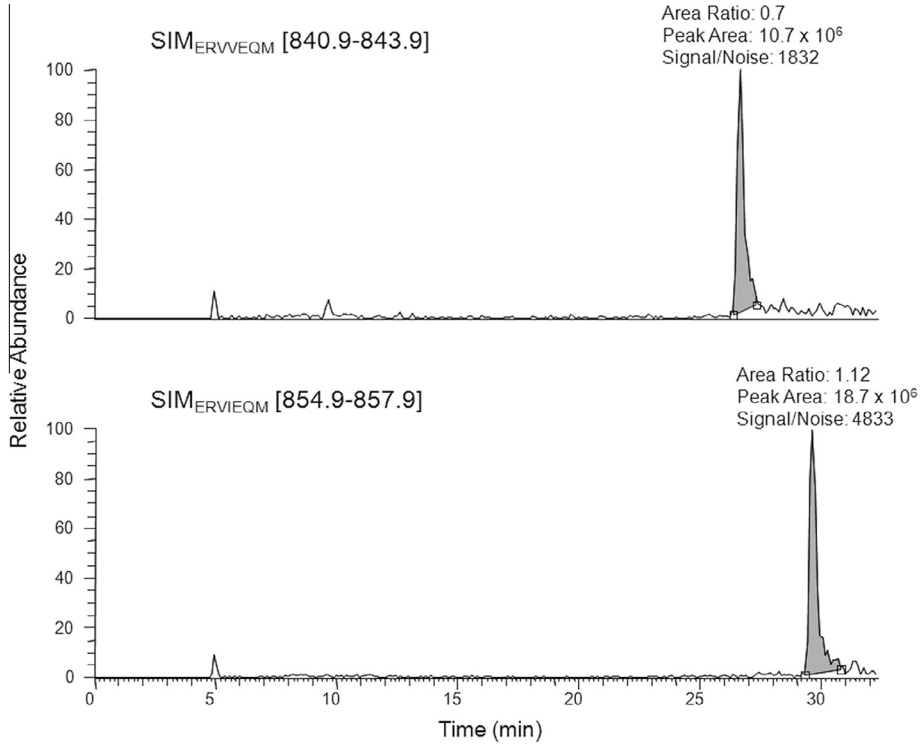

Fig. 3. Mass spectrometric detection of the human PrP^{27-30} allotypes isolated from the cerebral cortex of patient B. Detection of peptide ERVVEQM (upper panel) and ERVIEQM (lower panel) was simultaneously achieved by selectively monitoring parent ion currents (SIM mode) at *m*/*z* 840.9–843.9 and 854.9–857.9, respectively. Quantitative data are reported above SIM peak, as: (a) area ratio between the area of the endogenous PrP peptide and the spiked internal standard deuterated peptide; (b) peak area automatically achieved with same integration parameter; (c) signal to noise ratio.

A second possible mechanism is that the presence of a single amino acid substitution facilitates the formation of the first amyloid nucleus of PrP^{CJD}. In silico computer modelling and in vitro studies [20–22] with recombinant proteins showed that the R208H substitution destabilises the structure of PrP^{C} which may, in turn, facilitate the conversion into PrP^{CJD}. The effect of V210I mutation on the structure of the protein is less evident [20–22], but it may increase the stability of folding intermediates [23], or enhance supramolecular PrP^{CJD} aggregation [24], or induce the spontaneous misfolding of mutant PrP^{C} at the acidic pH of the endosomal compartments [25].

A third mechanism envisages that V210I and R208H mutations facilitate the interaction between mutant PrP^{C} and other organic [17,26] or inorganic [27,28] factors, which might be involved in the formation of the early steps of polymerization [29].

A higher resistance of mutant versus wild-type PrP^{CJD} to the cellular catabolic machinery can be also charged for the unbalanced ratio between the two allotypes however, this has never been demonstrated either for V210I or R208H PrP.

In a recent work, Zanusso and colleagues [30] investigated the presence of pathological PrP in brain tissue samples from P102L patients affected by GSS disease and found that a variety of "conformational quasispecies" of the pathological protein can be detected in tissue samples exposed to mild conditions of protease treatment. While these isoforms may have a diagnostic value, it is unknown whether they represent intermediate conformers towards the formation of protease-resistant and insoluble pathological PrP (such as partially folded and/or yet loosely aggregated monomers) and if they are also generated in TSE forms other than GSS. In our conditions of strong protease treatment and frequently repeated ultracentrifugation steps, it is high unlikely that not-fully developed pathological isoforms of PrP similar to those observed by Zanusso and colleagues [30] can contaminate the final fraction destined to MS analyses, therefore we can assume that only insoluble, aggregated, and PK resistant, fully-folded pathological isoforms of PrP contribute to the determination of mutant to wild-type ratio.

The issue of protein aggregation is central for the comprehension and treatment of a number of neurodegenerative disorders, including TSEs, Alzheimer's, and Parkinson's diseases. Several molecular models [31] have been proposed to describe the mechanism leading from monomeric precursors to misfolded proteins able to polymerize, yet, many uncertainties still persist, especially regarding the early mechanisms leading from monomeric precursors to misfolded proteins, the rate-determining steps, and its affecting factors.

In this context, the identification of the composition of amyloid aggregates is essential to refine the mechanistic models, particularly in the presence of mutant or polymorphic proteins where the definition of the allotypes involved is helpful to clarify the steps influenced by these primary structure variations. Until recently, however, analytical approaches developed for the determination of aggregated protein allotypes in human prion disorders, has provided only qualitative information [32,33] which are of limited utility for the refinement of protein aggregation models. Different mass spectrometry-based strategies for the relative quantification of PrP^{TSE} allotypes were already available to analyse the end-products of PrP pathological conversion in animal TSEs [14,34], but none of them had ever been applied to human TSEs up to now. The quantitative mass-spectrometry protocol successfully applied to gCJD in this study, far from being employed as a diagnostic PrP^{CJD} detection method, can be easily adapted to other genetic TSEs, by means of an accurate determination of the appropriate strategy (i.e. selection of adequate reporter peptides and supply of the corresponding calibrants and internal standards), as well as to other genetic proteinopathies, for investigating how the presence of mutations influences the molecular pathogenesis of the disease and ultimately susceptibility to disease, but also its clinical and pathological features [31,35].

Financial disclosure

This work was partially supported by the project Italia-Istituzioni USA 2010 ''Pathological & Biochemical features in prion-like induced protein-misfolding disorders''-Istituto Superiore di Sanità, by the project Ricerca Finalizzata 2009 (RF-2009-1474758) from the Italian Ministry of Health (to MP), and by Sapienza University grants (to MES and BM). The funders had no role in study design, data collection and analysis, decision to publish, or preparation of the manuscript.

Author contributions

Franco Cardone, Serena Principe, Bruno Maras, Maria Eugenia Schininà – conceived and designed the experiments. Maria Eugenia Schininà, Bruno Maras, Laura Di Francesco, Sabina Capellari, Piero Parchi, Silvio Notari, Anna Poleggi, Roberta Galeno, Ramona Vinci – performed the experiments. Franco Cardone, Serena Principe, Bruno Maras, Maria Eugenia Schininà – analyzed the data. Sabina Capellari, Piero Parchi, Silvio Notari, Vittorio Mellina, Susanna Almonti, Anna Ladogana – contributed reagents/materials/analysis tools. Franco Cardone, Serena Principe, Maurizio Pocchiari – wrote the paper. All authors read, revised and approved the final manuscript.

Acknowledgments

We are grateful to Dr Alessandra Garozzo and Mrs Cinzia Gasparrini for editorial assistance. This work is dedicated to the memory of our beloved colleague and friend professor Donatella Barra for her enthusiasm for science and life.

References

[1] A. Aguzzi, C. Sigurdson, M. Heikenwaelder, Molecular mechanisms of prion pathogenesis, Annu. Rev. Pathol. 3 (2008) 11–40.
[2] S. Capellari, F. Cardone, S. Notari, et al., Creutzfeldt–Jakob disease associated with the R208H mutation in the prion protein gene, Neurology 64 (2005) 905–907.
[3] G.G. Kovács, M. Puopolo, A. Ladogana, et al., Genetic prion disease: the EUROCJD experience, Hum. Genet. 118 (2005) 166–174.
[4] A. Ladogana, M. Puopolo, E.A. Croes, et al., Mortality from Creutzfeldt–Jakob disease and related disorders in Europe, Australia, and Canada, Neurology 64 (2005) 1586–1591.
[5] S. Mead, Prion disease genetics, Eur. J. Hum. Genet. 14 (2006) 273–281.
[6] M.S. Palmer, A.J. Dryden, J.T. Hughes, J. Collinge, Homozygous prion protein genotype predisposes to sporadic Creutzfeldt–Jakob disease, Nature 352 (1991) 340–342.
[7] M.W. van der Kamp, V. Daggett, The consequences of pathogenic mutations to the human prion protein, Protein Eng. Des. Sel. 22 (2009) 461–468.
[8] A. Ladogana, M. Puopolo, A. Poleggi, et al., High incidence of genetic human transmissible spongiform encephalopathies in Italy, Neurology 64 (2005) 1592–1597.
[9] C. Basset-Leobon, E. Uro-Coste, K. Peoc'h, et al., Familial Creutzfeldt–Jakob disease with an R208H-129V haplotype and Kuru plaques, Arch. Neurol. 3 (2006) 449–452.
[10] J.A. Mastrianni, C. Iannicola, R.M. Myers, et al., Mutation of the prion protein gene at codon 208 in familial Creutzfeldt–Jakob disease, Neurology 47 (1996) 1305–1312.
[11] S. Roeber, B. Krebs, M. Neumann, et al., Creutzfeldt–Jakob disease in a patient with an R208H mutation of the prion protein gene (PRNP) and a 17-kDa prion protein fragment, Acta Neuropathol. 109 (2005) 443–448.
[12] M.C. Silvestrini, F. Cardone, B. Maras, et al., Identification of the prion protein allotypes which accumulate in the brain of sporadic and familial Creutzfeldt–Jakob disease patients, Nat. Med. 3 (1997) 521–525.
[13] Y. Gu, S. Verghese, R.S. Mishra, et al., Mutant prion protein-mediated aggregation of normal prion protein in the endoplasmic reticulum: implications for prion propagation and neurotoxicity, J. Neurochem. 84 (2003) 10–22.
[14] C. Cartoni, M.E. Schininà, B. Maras, et al., Quantitative profiling of the pathological prion protein allotypes in bank voles by liquid chromatography–mass spectrometry, J. Chromatogr. B. Anal. Technol. Biomed. Life Sci. 849 (2007) 302–306.
[15] S.G. Chen, P. Parchi, P. Brown, et al., Allelic origin of the abnormal prion protein isoform in familial prion diseases, Nat. Med. 3 (1997) 1009–1015.
[16] V.A. Berardi, F. Cardone, A. Valanzano, et al., Preparation of soluble infectious samples from scrapie-infected brain: a new tool to study the clearance of transmissible spongiform encephalopathy agents during plasma fractionation, Transfusion 46 (2006) 652–658.
[17] A. Giorgi, L. Di Francesco, S. Principe, et al., Proteomic profiling of PrP27-30-enriched preparations extracted from the brain of hamsters with experimental scrapie, Proteomics 9 (2009) 3802–3814.
[18] G.G. Guilbault, M. Hjelm, Nomenclature for automated and mechanised analysis (Recommendations 1989), Pure Appl. Chem. 61 (1989) 1657–1664.
[19] D.S. Kirkpatrick, S.A. Gerber, S.P. Gygi, The absolute quantification strategy: a general procedure for the quantification of proteins and post-translational modifications, Methods 35 (2005) 265–273.
[20] K. Bamdad, H. Naderi-Manesh, Contribution of a putative salt bridge and backbone dynamics in the structural instability of human prion protein upon R208H mutation, Biochem. Biophys. Res. Commun. 364 (2007) 719–724.
[21] S. Liemann, R. Glockshuber, Influence of amino acid substitutions related to inherited human prion diseases on the thermodynamic stability of the cellular prion protein, Biochemistry 38 (1999) 3258–3267.
[22] J. Zuegg, J.E. Gready, Molecular dynamics simulations of human prion protein: importance of correct treatment of electrostatic interactions, Biochemistry 38 (1999) 13862–13876.
[23] A.C. Apetri, K. Surewicz, W.K. Surewicz, The effect of disease-associated mutations on the folding pathway of human prion protein, J. Biol. Chem. 279 (2004) 18008–18014.
[24] A.J. Thompson, K.J. Barnham, R.S. Norton, C.J. Barrow, The Val-210-Ile pathogenic Creutzfeldt–Jakob disease mutation increases both the helical and aggregation propensities of a sequence corresponding to helix-3 of PrP(C), Biochim. Biophys. Acta 1544 (2001) 242–254.
[25] I. Biljan, G. Ilc, G. Giachin, et al., Structural rearrangements at physiological pH: nuclear magnetic resonance insights from the V210I human prion protein mutant, Biochemistry 51 (2012) 7465–7474.
[26] E. Campisi, F. Cardone, S. Graziano, et al., Role of proteomics in understanding prion infection, Expert Rev. Proteomics 9 (2012) 649–666.
[27] S. Hesketh, A.R. Thompsett, D.R. Brown, Prion protein polymerisation triggered by manganese-generated prion protein seeds, J. Neurochem. 120 (2012) 177–189.
[28] S. Sorrentino, T. Bucciarelli, A. Corsaro, et al., Calcium binding promotes prion protein fragment 90-231 conformational change toward a membrane destabilizing and cytotoxic structure, PLoS ONE 7 (2012), http://dx.doi.org/10.1371/journal.pone.0038314.
[29] B. Caughey, G.S. Baron, B. Chesebro B, M. Jeffrey, Getting a grip on prions: oligomers, amyloids, and pathological membrane interactions, Annu. Rev. Biochem. 78 (2009) 177–204.
[30] S. Monaco, M. Fiorini, A. Farinazzo, et al., Allelic origin of protease-sensitive and protease-resistant prion protein isoforms in Gerstmann–Sträussler–Scheinker disease with the P102L mutation, PLoS ONE 7 (2012), http://dx.doi.org/10.1371/journal.pone.0032382.
[31] A.M. Morris, M.A. Watzky, R.G. Finke, Protein aggregation kinetics, mechanism, and curve-fitting: a review of the literature, Biochim. Biophys. Acta 1794 (2009) 375–397.
[32] F. Cardone, M. Pocchiari, Amyloidogenesis in transmissible spongiform encephalopathies, in: D.R.O. Morrison (Ed.), Prions and Brain Diseases in Animals and Humans, Plenum Press, New York, 1998, pp. 245–252.
[33] S. Principe, B. Maras, M.E. Schininà, et al., Unraveling the details of prion (con)formation(s): recent advances by mass spectrometry, Curr. Opin. Drug Discov. Devel. 11 (2008) 697–707.
[34] N. Morel, O. Andréoletti, J. Grassi, G. Clément, Absolute and relative quantification of sheep brain prion protein (PrP) allelic variants by matrix-assisted laser desorption/ionisation time-of-flight mass spectrometry, Rapid Commun. Mass Spectrom. 21 (2007) 4093–4100.
[35] B. Frost, M.J. Diamond, Prion like mechanisms in neurodegenerative diseases, Nat. Rev. Neurosci. 11 (2010) 155–159.